J Solid State Electrochem (2012) 16:1011–1018
DOI 10.1007/s10008-011-1440-6

ORIGINAL PAPER

High-efficiency ozone generation via electrochemical oxidation of water using Ti anode coated with Ni–Sb–SnO_2

Jalal Basiriparsa · Mahmoud Abbasi

Received: 1 January 2011 / Revised: 29 May 2011 / Accepted: 30 May 2011 / Published online: 29 June 2011

Abstract Ozone (O_3) has been generated on Ni–Sb–SnO_2/Ti electrode as anode immersed in acidic media at 25 °C by electrochemical process. The anode was electrochemically characterized by cyclic voltammetry and morphologically characterized by scanning electron microscopy (SEM) and X-ray diffraction. The concentration of dissolved ozone was determined by a UV/Vis spectrophotometer. The type of electrode with different times coating on the titanium mesh and different acid type and various concentrations (C_{acid}) were used, and the stability of the electrode was investigated under the experimental conditions by SEM images. Results shows that higher efficiency (53.7%) for O_3 generation by electrochemical oxidation of water were obtained in $HClO_4$ (1 M) and an applied potential of 2.4 V vs. Ag/AgCl in 150 ml volume undivided electrochemical cell.

Keywords Efficiency · Electrolysis · Ozone generation · Cyclic voltammetry · Stability

Introduction

Ozone (O_3) is one of the strongest oxidants used for disinfection, sterilization, green oxidation of pollutants, water and waste treatment, wood pulp bleaching, and chemical synthesis [1–5]. The extending of application is attributed to oxidizing properties of O_3. Ozone provides green oxidation since decomposition of ozone leads to environmentally friendly products (O_2) [6]. Electrochemical ozone production (EOP) has been much attended in the last decade because there are more advantageous than the classical corona discharge (CCD) technology [7–9]. The electrochemical method can generate a high current efficiency and high concentration of dissolved ozone and does not require high voltage [10].

Electrochemical ozone production is formed by electrolytic decomposition of water at the anode by two reactions (see Eqs. 1 and 2):

$$O_3 + 6H^+ + 6e^- \rightleftarrows 3H_2O \qquad E^\circ = 1.51\text{V vs.RHE} \quad (1)$$

$$O_3 + 2H^+ + 2e^- \rightleftarrows H_2O + O_2 \qquad E^\circ = 2.07\text{V vs.RHE} \quad (2)$$

Generation of ozone in electrochemical processes severely competes with O_2 evolution. Thermodynamically, oxygen evolution is strongly favored versus ozone production (Eq. 3):

$$O_2 + 4H^+ + 4e^- \rightleftarrows 2H_2O \qquad E^\circ = 1.23\text{V vs.RHE} \quad (3)$$

Thus, the inhibition of O_2 evolution is a first requirement for an efficient generation of O_3 at a reasonable current [4]. This can be achieved by suitable choice of the electrode material or the use of additives that partially inhibits the oxygen evolution reaction via blocking of its active sites [11]. Physical and chemical stabilities of electrode are the second requirement since the generation of O_3 needs a very high anodic potential. Thus, materials for electrochemical generation of ozone must have a high overpotential of oxygen evolution and should also be stable to strong anodic

J. Basiriparsa (✉) · M. Abbasi
Faculty of Chemistry, Applied Chemistry Department,
Bu-Ali Sina University,
Hamedan 65178, Iran
e-mail: parsa@basu.ac.ir

polarization in the electrolyte [10]. Various anodes have been studied for electrochemical ozone production such as: platinum, diamond, alpha- and beta-PbO_2, Pd, Au, dimensionally stable anode (DSA), glassy carbon, SnO_2–Sb_2O_5, and Ni–Sb–SnO_2 [1, 12–15]. Gold, DSA, and glassy carbon electrodes give low current efficiencies of <1% [8]. Platinum shows higher current efficiency from 6.5% to 35% but only at a very low temperature (−50 °C) and at the room temperature, the current efficiency fell to 0.5%. PbO_2 anodes can produce ozone at a current efficiency of 13% at room temperature, and for Ni–Sb–SnO_2 composite, coat on Titanium mesh shows higher current efficiency of ozone production (>36.5%) [10–16].

In this research, we gained a high coulombic efficiency of ozone production by electrochemical method using Ti mesh anode coated with Ni–Sb–SnO_2 in 150 ml volume undivided electrochemical cell. Several parameters have been optimized, such as coating times effect, electrolyte type, electrolyte concentration, and applied voltage. Finally, we investigated stability of electrode by observation and comparison of SEM images before and after electrolysis. The anode was electrochemically characterized by cyclic voltammetry (CV) and morphologically characterized by scanning electron microscopy (SEM) and X-ray diffraction (XRD).

Experimental

The concentration of dissolve ozone was determined by UV/Vis spectrophotometer (Jusco, Japan), and the ozone in the gas phase had not been measured. The UV spectrum was calibrated by the standard indigo method [17]. For the spectrophotometer, using 1 mg L^{-1} dissolved ozone gave an absorbance of 0.098 at the wavelength of 258 nm. The coulombic efficiency (CE) of the ozone generation was determined from the following equation (Eq. 4) [18]

$$\mathrm{CE}\% = \frac{n_{\mathrm{Exp}}}{n_{\mathrm{th}}} = \frac{6Fn_{\mathrm{Exp}}}{Q_{\mathrm{th}}} \times 100 \qquad (4)$$

where n_{Exp} and n_{th} (Q_{th}/zF) are the number of moles of O_3 obtained experimentally (0.098×absorption at the wavelength of 258 nm) and calculated theoretically, respectively; z is the number of electrons (equals six in the present case, see Eq. 1); and Q_{th} equals $i \times t$ (where i is the current applied for a time period t).

The electrodes were prepared by thermal coating of Ni–Sb–SnO_2 on a titanium mesh (Ti) substrate with an absolute ethanol solution containing $SnCl_4 \cdot 5H_2O$ (98%, Sigma Aldrich), $SbCl_3$ (99.5%, Merck), and $NiCl_2 \cdot 6H_2O$ (98%, Merck) precursors followed by pyrolysis at 520 °C. The preparation procedure is near the same as described in Cheng and Chan [19] and Wang et al. [10]. For making an electrode, 2.5×2.5 cm titanium screen spot-welded with a 1 mm diameter Ti wire was treated in 10% boiling oxalic acid for 1 h for two times, washed with distilled water, and dried naturally. The pyrolysis solution was prepared as consists of Ni–Sb–SnO_2 in the molar ratio of 500:8:1 [10, 19]. Each mesh electrode is dipped into the coating solution for 30 s, stirred around for 30 s (1 min), and then transferred to an oven at 105 °C for 15 min, and in continuance, the electrodes were annealed in furnace to 520 °C for 25 min. The dip-coating and pyrolysis procedure was repeated 12 times. In the final heating step, the electrodes were annealed at 520 °C for a longer duration of 1 h.

A commercial saturated Ag/AgCl electrode from Metrohm as reference electrode and platinized titanium (electrodeposition of H_2PtCl_6 on the Ti mesh (2.5×2.5 cm)) as counter electrode were used. The volume of electrochemical cell was 150 ml. Electrolysis experiments were carried out in three-electrode technique with constant potential coulometer (coulometer 2050, Behpajooh Company, Iran; Fig. 1).

SEM observation was performed on LEO 1455 VP (LEO Electron Microscopy, Ltd) scanning microscope. The cyclic voltammetry experiments were conducted using a three-electrode cell, with platinum wire as the counter electrode, Ag/AgCl as the reference electrode, and Ni–Sb–SnO_2/Ti electrode (1×1 cm) as the working electrode. CV curves of the testing anodes were produced by potentiostat/galvanostat ATOLABS (Netherlands).

X-ray diffraction (XRD) patterns of the coating films on these electrodes were recorded on an XRD instrument (Ital structure APD 2000, Italy), using Cu K_{alpha} radiation, with an operating voltage of 40 kV and current of 30 mA.

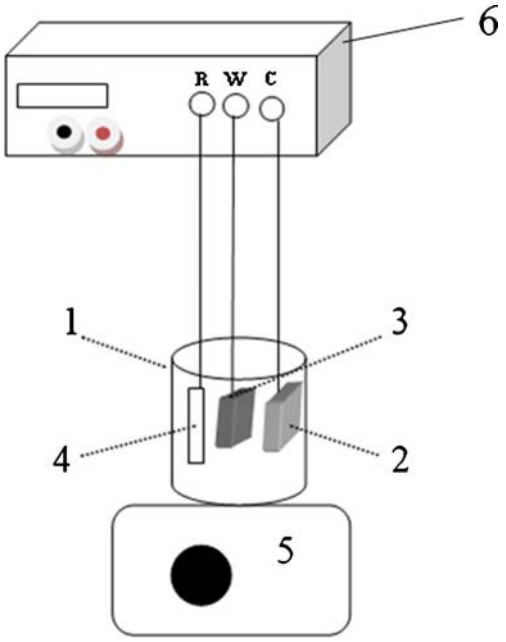

Fig. 1 Electrochemical set up. *1* Electrochemical cell. *2* Counter electrode. *3* Working electrode. *4* Reference electrode. *5* Magnetic stirrer. *6* Coulometer

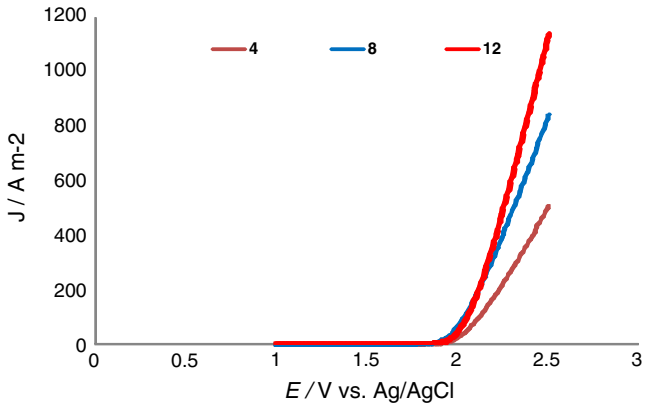

Fig. 2 Anodic polarization curves at different coating times (4th, 8th, 12th) of Ni–Sb–SnO_2; C_{HClO4}=1 M; potential scan rate, 50 mV s^{-1}

Results and discussion

Characterization of the electrodes

The cyclic voltammograms of the anode was shown in Fig. 2 The cyclic voltammetry was performed at 50 mV s^{-1} in 1 M $HClO_4$ at room temperature. The onset potential is 2 V vs. Ag/AgCl, and it was much higher than the typical value expected for oxygen evolution in acid solution which is 1.02 V vs. Ag/AgCl, indicating that oxygen evolution was kinetically suppressed. Within the scanned voltage range, CVs of the electrodes did not have any peaks or shoulders. There was no cathodic current on the reverse scan, and consecutive CV scans were reproducible.

The electrode surface was observed with a scanning electron microscopy (SEM). Figure 3 shows representative SEM images of the anode electrode with different coating times. Images show that with increasing of coating times, the coverage of surface increased and it caused increasing of active sites in electrode surface.

From the XRD profiles in Fig. 4, all the doped SnO_2 coating showed the same cassiterite tin dioxide, and the obvious X-ray diffraction peaks of SnO_2 are highlighted in the figure. There are obvious antimony oxide and nickel oxide peaks that appear, which indicates that the antimony and nickel have weak intensity. It may be that the antimony and nickel are incorporated into the SnO_2 lattice to form solid solution.

Electrochemical ozone production

The concentration of dissolved ozone was determined by a UV/Vis spectrophotometer, and 1 mg L^{-1} dissolved

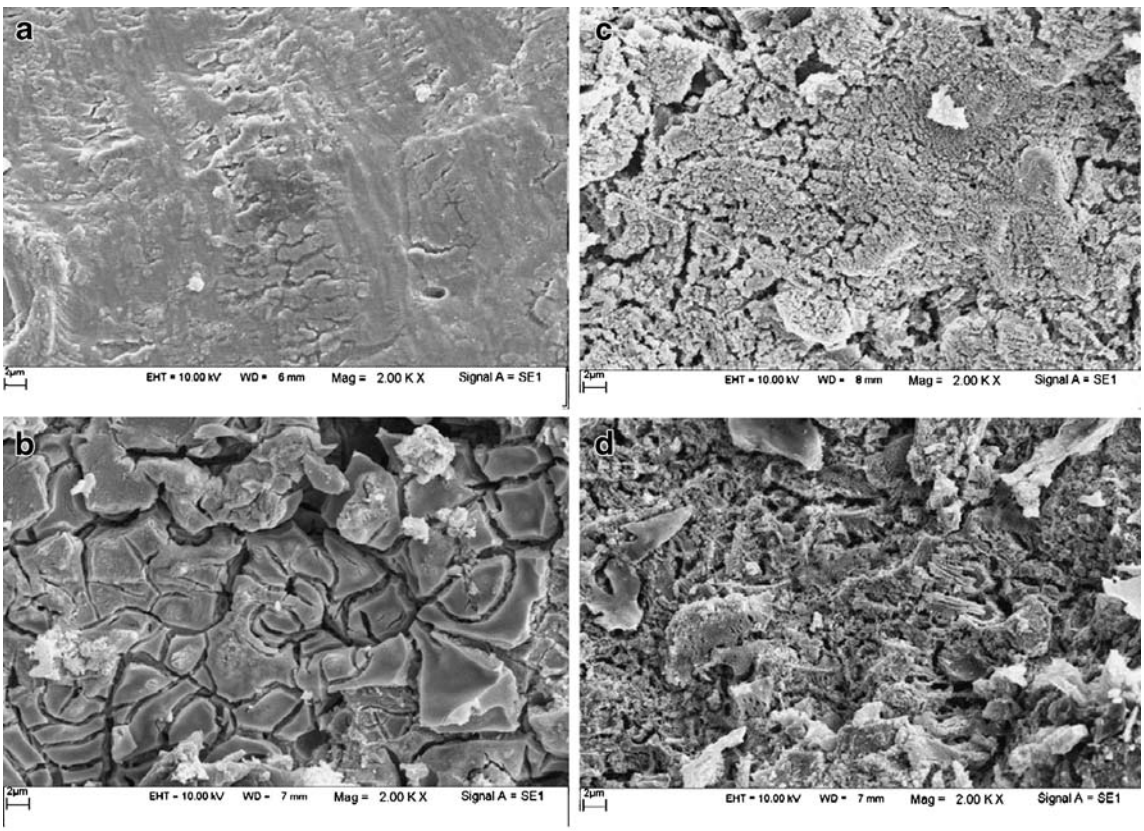

Fig. 3 SEM images of different coating times of Ni-Sb-SnO_2: **a** surface of net titanium without coating, **b** 4th coating times, **c** 8th coating times, **d** 12th coating times

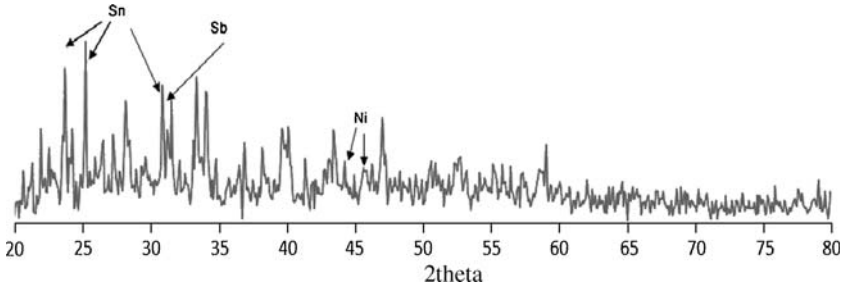

Fig. 4 XRD pattern of Ni–Sb–SnO_2 1:8:500

ozone gave an absorbance of 0.098 at the of wavelength 258 nm. The UV spectrum was calibrated by standard indigo method [17]. Figure 5 shows UV spectrum of ozone with the gradual increase of the ozone UV peak. The first spectrum was collected after 1 min of electrolysis. The peak absorbance increases with electrolysis time because the ozone concentration increases with during electrolysis.

As shown in Fig. 6, a steady-state aqueous ozone concentration was reached after 20 min (1,200 s) at 2.4 V vs. Ag/AgCl and different concentration of $HClO_4$.

The dissolved ozone concentration depended on the applied voltage, concentration, and type of electrolyte. Result shows that the concentration of ozone vary in the range of 2 mg L^{-1} to above 27 mg L^{-1} at the experimental condition. These values of dissolved ozone are more than necessary concentration for most applications and are usually not attainable in the conventional CCD process [20]. Figure 6 is shown in aqueous ozone concentration.

Effect of electrode coating times

Titanium electrode has a high oxygen evolution overpotential >1.8 V vs. Ag/AgCl. Ozone production could not be detected from a titanium anode even at higher potentials. The applied potential which at electrolysis experiment was conducted (2.4 V vs. Ag/AgCl) and revealed that titanium substrate may have a small effect on efficiency, since more oxygen may be generated on titanium. Electrochemical ozone production depended on the amount of the active coating materials. Figure 3 shows the effect of coverage of titanium substrate, and the amount of active coating materials (Ni–Sb–SnO_2) was investigated by comparing the performance of electrodes with different times of coatings. A fixed amount of the precursor solution composed of Sn/Sb/Ni=500:8:1 was deposited in each coating step and pyrolyzed at 520 °C [10, 19]. Ozone coulombic efficiencies were determined by the electrolysis in 1 M $HClO_4$ under a constant potential of 2.4 V vs. Ag/AgCl. Figure 7a shows that the CE increased steadily with the increasing active material coating times from 4 to 12 and that each coating has positive effect on ozone production. Figure 7b shows that the maximum CE was obtained for all coating times at 60 s of electrolysis. This indicated that with 12th coatings, either the titanium substrate was fully covered or the utilization of the doped SnO_2 material has reached the maximum and caused increasing of active site in surface electrode.

The tin dioxide is a semiconductor in which the oxygen vacancies would donate electrons to its conduction band [21]. Also, antimony(V) as donor (energy level ED) would be donating electrons to the conduction band; thus, it could increase the conductivity by increasing the charge carrier

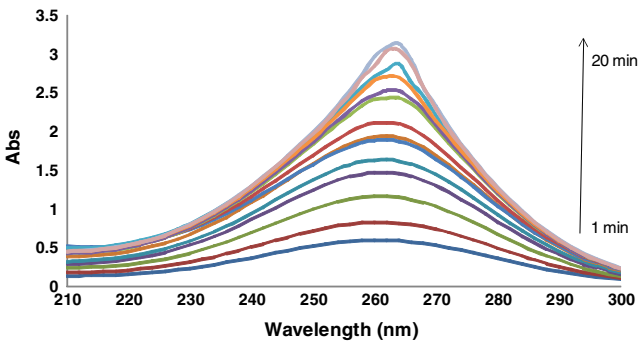

Fig. 5 UV spectra solution with dissolved ozone concentration, applied voltage=2.4 V vs. Ag/AgCl, C_{HClO4}=1 M

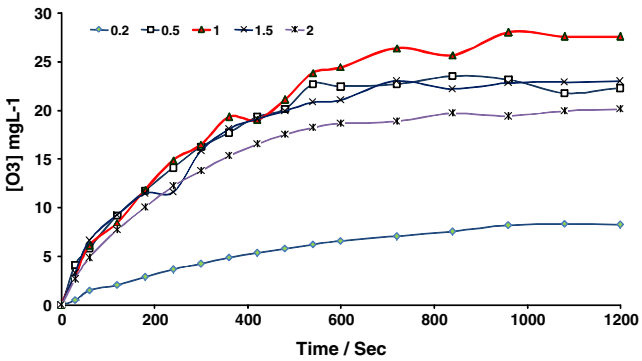

Fig. 6 Ozone concentrations in water vs. the electrolysis time at different concentration of $HClO_4$. O_3 was generated applying a constant potential of 2.4 V vs. Ag/AgCl

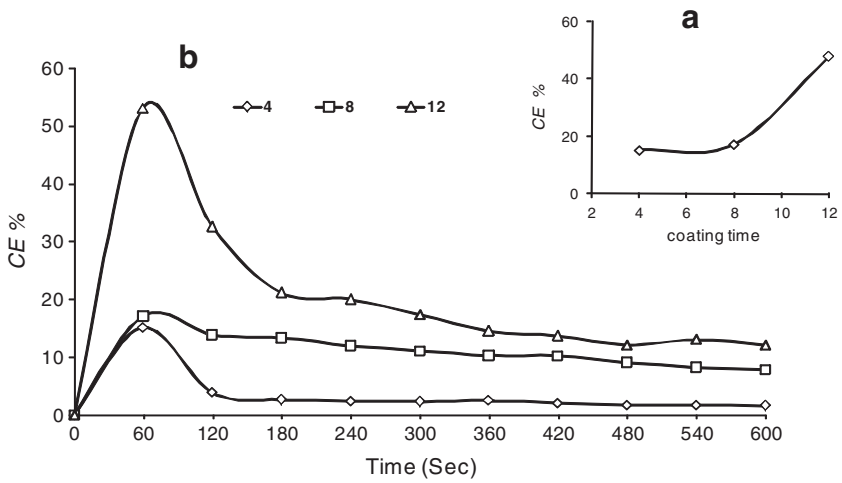

Fig. 7 Effect of coating times on O_3 electrogeneration efficiency. Applied voltage= 2.4 V vs. Ag/AgCl and C_{HClO4}= 1 M. **a** 60 s and **b** during electrolysis

density. Nickel(III) due to its lower valence than tin(IV) functioned as acceptor (energy level EA) and would introduce positively charged holes in the valence band by accepting electrons from the bulk. The band diagrams for donor and acceptor are illustrated in Fig. 8.

The electrons donated by antimony(V) and oxygen vacancies could be well compensated with the holes generated by nickel(III), and around the nickel site would be negatively charged. This negative charge would be trapped by adsorbed oxygen, that is, the oxygen would be strongly absorbed around Nickel site. The negative charge around the nickel(III) would distribute more uniformly and decrease the oxygen absorption. While after donating out electrons, the antimony(V) sites would be positively charged and were always considered as the Lewis acid sites, on which water may be oxidized to OH free radicals [22] and dioxygen may be formed quickly. In this process, on the antimony- and nickel-doped tin oxide electrode, due to the adjacent nickel site available, the dioxygen formed on antimony(V) will be transferred to and then adsorbed on nickel site as an intermediate. The adsorbed dioxygen will react further with the hydroxyl free radical on adjacent antimony site to form HO_3 radical, which would be quickly oxidized to ozone by deprotonation. Figure 9 shows the mechanism for ozone generation on Ni–Sb–SnO_2-coated Ti electrode.

Effect of applied voltage

The effect of applied voltage on the CE of ozone production is shown in Fig. 10. The results showed that an optimal potential of 2.4 V vs. Ag/AgCl with the highest CE of 53.7% was at 60 s and then it has declined to below 20% at 600 s for 1 M $HClO_4$. Figure 10a shows the CE decreased after 2.4 V at 60 s, and also, Fig. 10b shows decreased of CE during electrolysis time. The decline of the CE may be from either an increase of the competing side reaction of oxygen evolution or increase in ohmic losses due to lower conductivity in the solution when gas bubbles were generated also from inactivation and instability of reaction sites.

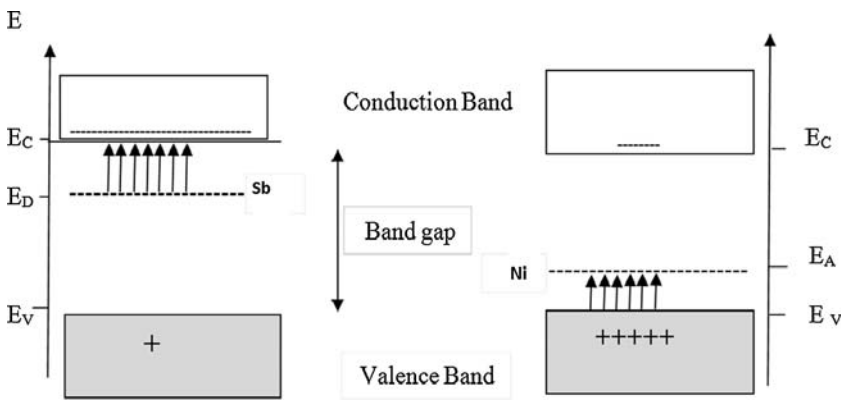

Fig. 8 Band energy of diagram for semiconductor

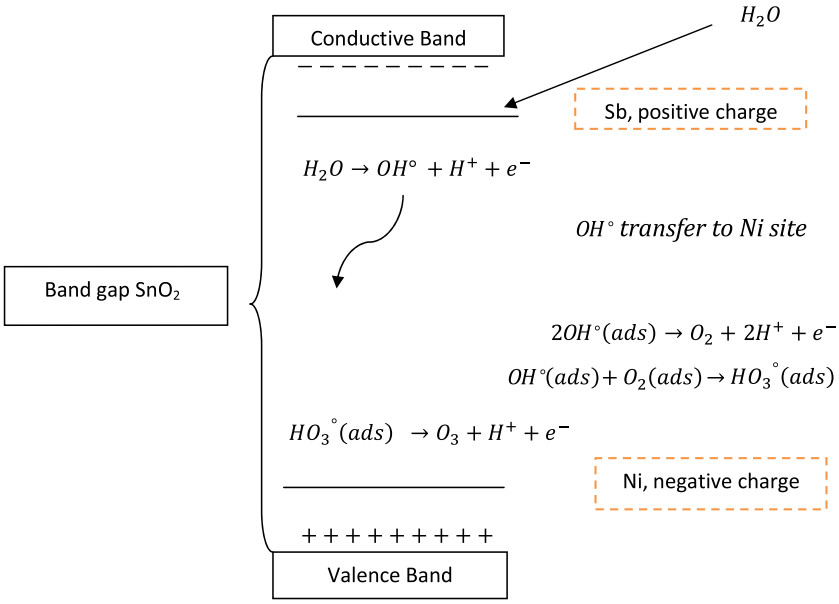

Fig. 9 Mechanism for ozone generation on Ni–Sb–SnO_2/Ti electrode

The effect of acid type and concentration

Ozone electrochemical production efficiency was found to differ in various acidic media and concentrations [4]. The concentration of acid would directly affect proton concentration. The type of acid anions had important effect—it evidently affected the selective adsorption of water on electrodes. The effect of the acid type and concentration on CE of ozone production was investigated. Three acids—perchloric acid, sulfuric acid, and phosphoric acid—were used, representing different valence charges anions. Figure 11 shows that the effect of acid concentration was similar for the three types of acids. Highest current efficiency was obtained at 60 s, and overall current efficiencies for $HClO_4$, H_2SO_4, and H_3PO_4 were, respectively, 20.07%, 17.55%, and 9.01%. The type of anion had a large effect on ozone production. The highest coulombic efficiency was achieved in $HClO_4$ where lower efficiency was found in H_3PO_4.

The main reaction of H_2SO_4 is the formation of peroxodisulfuric acid due to oxidation of the sulfuric acid as supporting electrolyte [23, 24]. In contrast, the main reaction of $HClO_4$ is oxygen evolution due to water oxidation (see Eqs. 5 and 6).

$$2H_2SO_4 \rightarrow H_2S_2O_8 + 2e^- + 2H^+ \quad (5)$$

$$2H_2O \rightarrow O_2 + 4e^- + 4H^+ \quad (6)$$

Figure 12 shows the results of voltammetric measurements and bulk electrolysis with Ni–Sb–SnO_2 in 1 M $HClO_4$, 1 M H_2SO_4, and 1 M H_3PO_4, where the main reaction products are different (O_2 in $HClO_4$ and perox-

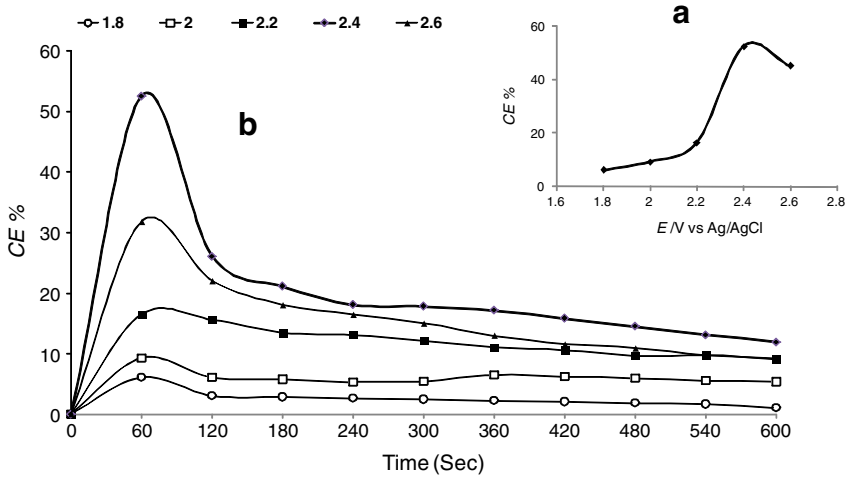

Fig. 10 Effect of applied voltage on O_3 electrogeneration efficiency. C_{HClO4}=1 M. **a** 60 s and **b** during electrolysis

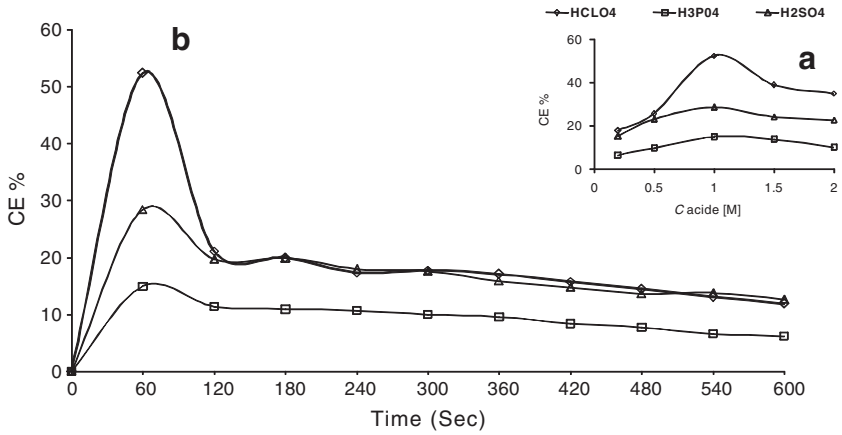

Fig. 11 Effect of acid type and concentration on CE. Applied voltage=2.4 V vs. Ag/AgCl. **a** 60 s and **b** during electrolysis

odisulfuric acid in H_2SO_4). In order to explain this behavior, a simplified model is proposed for water oxidation on Ni–Sb–SnO_2. At the same potential, the current density by H_2SO_4 and H_3PO_4 is shifted to lower current densities compared with the $HClO_4$. This means that the H_3PO_4 and H_2SO_4 inhibited the oxygen evolution.

Stability of electrode

When electrochemical ozone production is used in acidic media and high anodic potential, the stability of the electrode is important. The stability of the Ni–Sb–SnO_2/Ti electrode was examined by taking SEM before (Fig. 13a) and after (Fig. 13b) being used for ozone electrochemical production for 3 h.

Observation and comparison of SEM images demonstrated that little change occurred on the surface of electrode after 3 h of electrolysis. Also, the results show that coulombic efficiency was almost fixed after 180 s in all condition (Figs. 7, 10, and 11).

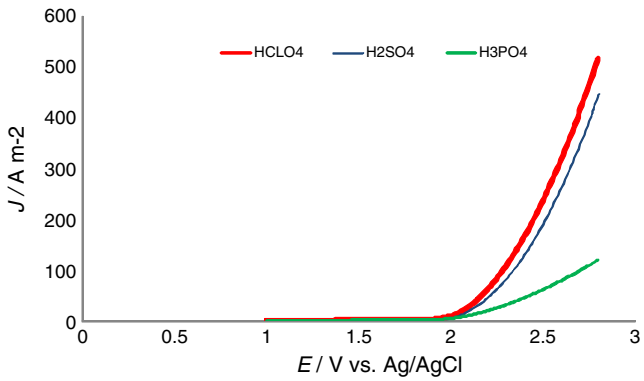

Fig. 12 Anodic polarization curves at different electrolyte. Potential scan rate, 50 mV s^{-1}

Conclusions

Ozone was generated with high coulombic efficiency via electrochemical oxidation of water on Ni–Sb–SnO_2/Ti

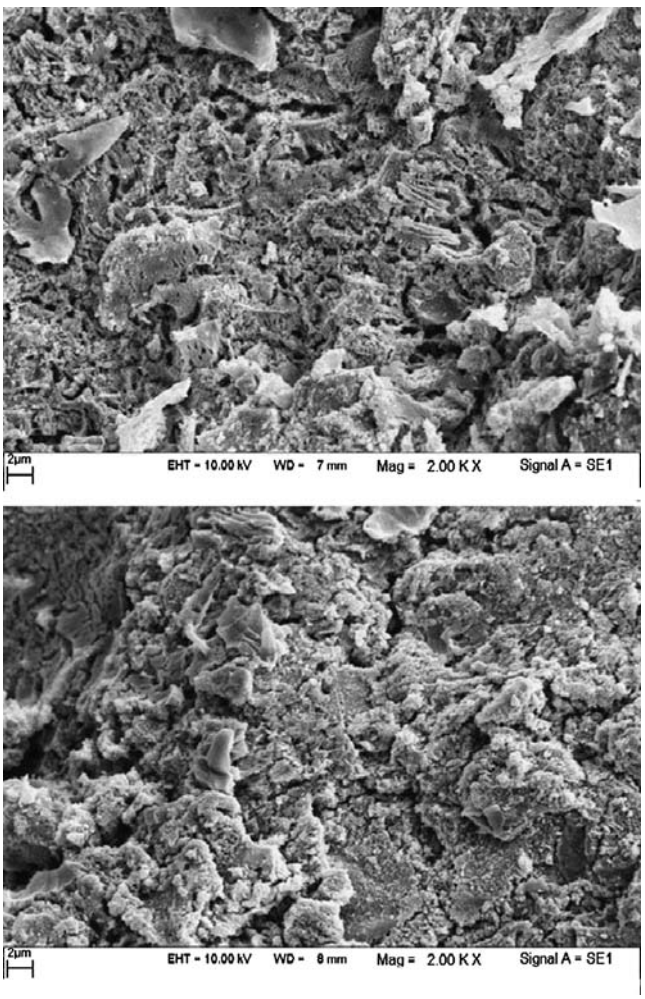

Fig. 13 Scanning electron micrograph obtained for Ni–Sb–SnO_2/Ti electrode **a** before and **b** after being used for electrolysis for 3 h at constant potential of 2.4 V in 1 M $HClO_4$

electrode at different operating condition. The electrode was characterized by CV, SEM, and XRD. Higher efficiency of EOP was obtained at 2.4 V vs. Ag/AgCl in 1 M $HClO_4$. The efficiency of ozone generation was 53.7%. Observation and comparison of SEM images before and after electrolysis demonstrated relative stability of anode surface.

References

1. Arihara K, Terashima C, Fujishima A (2007) J Electrochem Soc 154:E71–E75
2. Pichet P, Hurtubise C (1975) Proceedings of second international symposium on ozone technology, Montreal, Canada, 11–14 May, 1975
3. Meng MX, Hsieth JJ (2000) Tappi J 83:67–72
4. Da Silva LM, De Faria LA, Boodts JFC (2003) Electrochim Acta 48:699–709
5. Stucki S, Theis G, Kötz R, Devantay H, Christen H (1985) J Electrochem Soc 132:367–371
6. Awad MI, Sata S, Kaneda K, Ikematsu M, Okajima T, Ohsaka T (2006) Electrochem Commun 8:1263–1269
7. Santana MHP, De Faria LA, Boodts JFC (2004) Electrochim Acta 49:1925–1935
8. Foller PC, Tobias W (1982) J Electrochem Soc 129:506–515
9. Chernik AA, Drozdovich VB, Zharskii IM (1997) Russ J Electrochem 33:259–264
10. Wang YH, Cheng S, Chan KY, Li XY (2005) J Electrochem Soc 152:D197–D200
11. Da Silva LM, De Faria LA, Boodts JFC (2001) Pure Appl Chem 73:1871–1884
12. Tatapudi P, Fenton JW (1993) J Electrochem Soc 140:3527–3530
13. Foller PC, Tobias W (1981) J Phys Chem 85:3238–3244
14. Chen QY, Shi DD, Zhang YJ, Wang YH (2010) Water Sci Technol 62:2090–2095
15. Lipp L, Pletcher D (1997) Electrochim Acta 42:1091–1099
16. Christensen PA, Lin WF, Christensen H, Imkum A, Jin JM, Li G, Dyson CM (2009) Ozone Sci Eng 31:287–293
17. Bader H, Hoigne J (1981) Water Res 15:449–456
18. Awad MI, Saleh MM (2010) J Solid State Electrochem 14:1877–1883
19. Cheng SA, Chan KY (2004) Electrochem Solid State Lett 7:D4–D6
20. Fernando JB (2004) Ozone reaction kinetics for water and wastewater systems. Lewis, Boca Raton
21. Jolivet JP (2000) Metal oxide chemistry and synthesis: from solution to oxide. Wiley, New York
22. He D, Mho S (2004) J Electroanal Chem 568:19–27
23. Michaud PA, Mahe E, Haenni W, Perret A, Comninellis Ch (2000) Electrochem Solid State Lett 3:77–79
24. Michaud PA, Panniza M, Outattara L, Daiaco T, Foti G, Comninellis Ch (2003) J Appl Electrochem 33:151–154